Journal of Ovonic Research Vol. 12, No. 2, March - April 2016, p. 87 - 93

EFFECT OF NEODYMIUM SUBSTITUTION ON STRUCTURAL, OPTICAL, MAGNETIC AND ANTIBACTERIAL ACTIVITY OF ZINC SELENIDE NANOPARTICLES

N. PRIYADHARSINI[a], M. THAMILSELVAN[a*], S. SANGEETHA[b], S.VAIRAM[b]
[a]*Department of Physics, Thanthi Periyar Government institute of technology, Vellore, India*
[b]*Department of Chemistry, Government college of technology, Coimbatore, India*

ZnSe and neodymium doped ZnSe ($Zn_{1-x}Nd_xSe$) with x=0, 0.05, 0.07 and 0.10 precipitated nanoparticles at pH 5 were synthesized through wet chemical route. XRD studies reveal the prepared nanoparticles have cubic zinc blende structure and the particle size is in the range of 5-30 nm. The SEM micrograph analysis the surface of the sample, it visibly reveals nanophase formation and no trace of the oxide and purity of the synthesized samples is confirmed by EDAX analysis. Strong absorption in the visible region of the electromagnetic spectrum is examined by UV-Vis spectrum and optical band gap decrease with dopant concentration. The magnetic hysteresis study was carried out using VSM and it shows soft magnetic nature. The antibacterial properties of the nanoparticles against gram positive and gram negative bacterial strain were determined using disc diffusion method.

(Received February 10, 2016; Accepted April 6, 2016)

Keywords: neodymium, VSM, XRD, energy gap

1. Introduction

The recognition of the size and shape dependent physical and chemical properties of semiconductor nanostructures and their doped form has stimulated the scientific efforts towards the assembly of nanocrystals in control way [1][2][3]. Transformation of materials from bulk to nanodimensional state attributes unique photo-physical properties. Also, decrease in particle size results in high surface to volume ratio, which accelerate the chemical reactions and photon absorption in the surface active sites. Introducing an impurity atom into a semiconductor host matrix depends on the properties such as energy gap value and equivalent ionic radius of the host and dopant ions [4][5]. Zinc Selenide (ZnSe) is an n-type, direct wide band gap (~2.8 eV) semiconductor material has a room temperature Bohr radius and large exciton binding energy of 3.8 nm and 21 MeV respectively. Chemically synthesized nanostructures are of primary importance due to their unique properties and pertain their potential application in nanoelectronics [6], nano-Optronics [7], nanosensors [8], high-density optical storage [9] and biomedical sensors. There are several reported preparation methods for ZnSe, namely, physical vapor deposition [10], pyrolysis technique [11], hydrothermal method [12], solvothermal method [13], electrodeposition [14] and wet chemical precipitation method [15]. Among all, wet chemical precipitation has many advantages, includes cost effectiveness, particle stability, versatility, less complexity. Herein, we demonstrate the successful synthesis of uniform, nearly monodispersed nanoparticles by wet chemical protocol. The paper deals with the synthesis of neodymium doped ZnSe nanoparticles and the accounted results suggested that this system is suitable for fabrication of nanoelectronics devices, as absorber layer in DSSC and biomedical sensors.

* Corresponding author: prsr72@gmail.com

2. Experimental method

2.1 Preparation of precipitate powder

Neodymium doped ZnSe samples ($Zn_{1-x}Nd_xSe$) with x=0, 0.05, 0.07 and 0.10 at pH 5 were prepared by wet chemical precipitation technique, adding hydrazine hydrate as the precipitating agent at room temperature. Freshly prepared aqueous solution of analytical grade zinc nitrate ($Zn(NO_3)_2$), neodymium oxide (Nd_2O_3) and selenium dioxide (SeO_2) were used as precursor materials. Initially, 2 g of zinc nitrate and 0.555 g selenium dioxide were separately dissolved in 60 ml of double distilled water in three neck round bottom flask and stirred for 30 min. For dopant precursor, Convert neodymium oxide into nitrate by adding 2N nitric acid in a water bath to avoid oxide peaks in the final product. The freshly prepared dopant solution was added in Zinc nitrate solution with constant stirring until pale violet color turbid free solution is reached. The precipitation process was carried by drop wise addition of selenium dioxide into the zinc nitrate solution under vigorous stirring, followed by addition of hydrazine hydrate to fix the pH and allowed to stir for 12 hrs. The resultant precipitate was centrifuged at 4000 rpm/min and washed thoroughly with double distilled water and acetone. The collected residue was allowed to dry at room temperature and preserved in an airtight container.

2.2 Antibacterial assay

The inoculum for the experiment were arranged in fresh Nutrient broth and standardized by adjusting the turbidity of the culture to that of McFarland standards. The standardized inoculum is inoculated in the plates with the lid closed and dried at room temperature. Each Petri dish is divided into 4 parts, in each part samples such as ($Zn_{1-x}Nd_xSe$) x=0, 0.05, 0.07 and 0.1 in 100µg (discs are soaked overnight in SAMPLE solution) and standard Ciprofloxacin 10µg, placed in the center of the plate with the help of sterile forceps. Then Petri dishes are placed in the refrigerator at 4º C for 1 hour for diffusion and Incubate at 37 ºC for 24 hours. Observed the zone of inhibition of the samples and the control, measured using a meter scale and record the average of two diameters of each zone of inhibition.

2.3 Characterization

The structural and phase purity of the end product was done by XRD analysis using XPERT-PRO diffractometer at the scanning rate of 0.02°/min for the range from 10° –80° using Cu K_α source. Scanning electron micrographs (SEM) was recorded on SEMJEOL JAX-840A electron micro analyzer with an operating voltage 200 kV which was also equipped with Energy Dispersive X-ray (EDAX) photometer. The optical properties of the as prepared Nd doped ZnSe nanomaterials were evaluated by UV-VIS spectroscopy using JASCO V-570 Spectrophotometer ranging between 200 nm to 1500 nm at the slit width of 1 nm. The ZnSe doped with Nd^{3+} were studied for magnetic hysteresis with Lakeshore- USA model 7404 vibrating sample magnetometer.

3. Results and discussion

3.1 Structural and compositional analysis

X-ray diffraction spectra of synthesized undoped ZnSe and $Zn_{1-x}Nd_xSe$ (x= 0.05, 0.07 and 0.1) nanopowder samples are shown in fig. 1. Undoped and $Zn_{1-x}Nd_xSe$ (x=0, 0.05, 0.07 and 0.1) have a cubic zinc blende structure with major reflection planes at (1 1 1), (2 2 0) and (3 1 1). The peaks are well consistent and match with standard JCPDS no. 80-0021and lattice constant value is a=5.634 Å. The crystallite size of the samples is calculated from full width half maximum (FWHM) of prominent peaks using the Debye-Scherrer formula [16] [17],

$$D = \frac{0.9\,\lambda}{\beta\,cos\theta}$$

Where D is the average crystallite size, λ is the wavelength of X-ray radiation (1.5405 Å), β is full width at half maximum and θ is the Bragg angle. Calculated crystallite size for undoped ZnSe is 4.7 nm and 11.3 nm, 16.8 nm and 26.5 nm for $Zn_{1-x}Nd_xSe$ (x= 0.05, 0.07, 0.10) respectively. No other impurity phases and secondary phase formation of SeO_2, NdO_3 are detected in the XRD spectra, this indicates the purity of the sample and Nd ions has been doped into the ZnSe host lattice. As dopant concentration increases, particle size and d-spacing value increases and the intensity of peak decreased. This may be due to substitution of larger ionic radius Nd^{3+} (0.983 Å) in smaller ionic radius Zn^{2+} (0.74 Å).

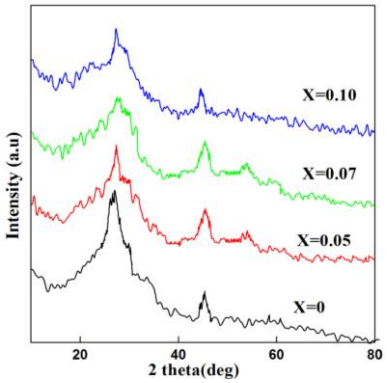

Fig. 1 XRD pattern of $Zn_{1-x}Nd_xSe$ Nanoparticles

The chemical composition of the nanopowders was investigated by energy dispersive X-ray spectrum are shown in Fig. 2. It confirms the expected presence of elements Zn, Se and Nd in the stoichiometry weight percentage without any impurities.

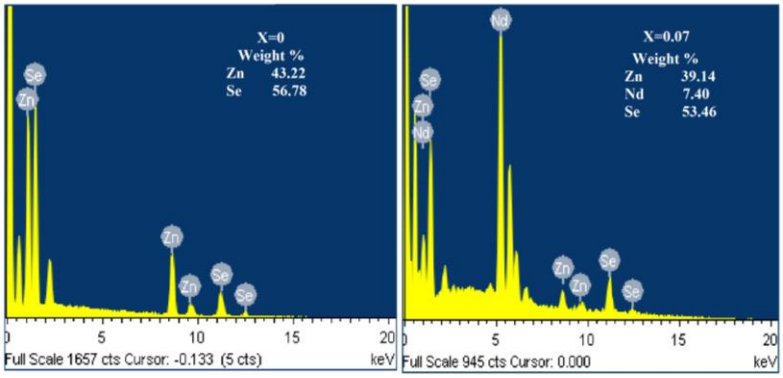

Fig. 2 EDAX spectra of ZnSe and $Zn_{0.93}Nd_{0.07}Se$ Nanoparticles

3.2 SEM analysis

The SEM micrographs of undoped ZnSe and $Zn_{1-x}Nd_xSe$ (x= 0.05, 0.07 and 0.1) at pH 5 is shown in Fig. 3(a-d) respectively. The SEM image shows fine powder and sponge like structure with porosity. The average particle size is calculated using line section method and it in the range of 15-35 nm. As the dopant Nd^{3+} concentration increases the structure becomes porous and crystallite size is increased as explain in XRD analysis. This may be due to replace of Zn^{2+} ions with Nd^{3+} ions promote the grain growth and agglomeration is reduced with dopant concentration.

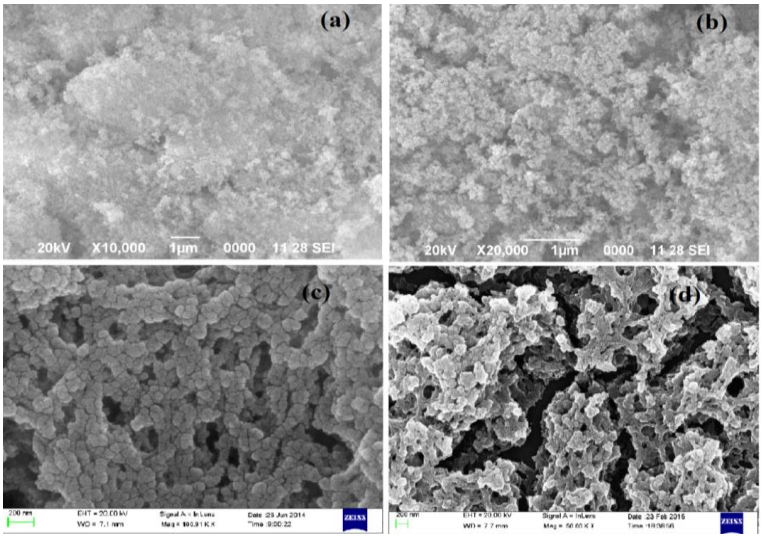

Fig. 3 SEM micrograph of $Zn_{1-x}Nd_xSe$ (a) X=0, (b) X=0.05, (c) X=0,07 and (d) X=0.10 Nanoparticles

3.3 Optical analysis

The UV-Vis absorption and reflectance spectra of ZnSe:Nd nanoparticles were recorded at room temperature in the range of 200 to 1500 nm are presented in Fig. 4.a and 4.b. For pure and doped ZnSe nanoparticles have a strong absorption edge is noted in the visible region centered at 577 nm and the absorption edge shifts towards lower wavelength with an increase of Nd content, indicating band gap narrowing. It is the expected characteristics of the layer for the fabrication of dye sensitized solar cell (DSSC).

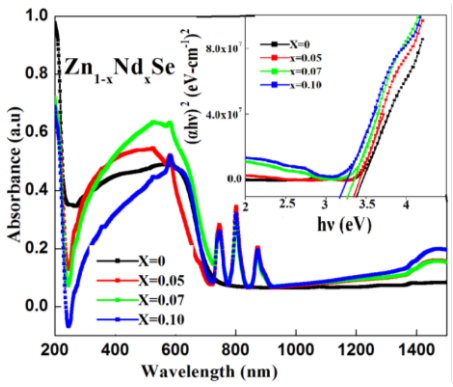

Fig. 4.a UV-Vis absorbance spectra (inset: $(\alpha h\nu)^2$- hν curve) of $Zn_{1-x}Nd_xSe$ Nanoparticles

Excitation of electronic transition from valance to conduction band gives band gap value. The optical band gap can be estimated from $(\alpha h\nu)^2$ Vs hν plot from absorption spectra [18] are shown in Fig. 4.a (Inset). ZnSe is a direct band gap system which shows linear behavior and the energy gap value for ZnSe is 3.41 eV, is higher than bulk ZnSe (2.8 eV) [19] [20] is due to electron hole confinement effect [21]. As Neodymium dopant increases, the band gap value is found to be 3.38 eV, 3.26 eV and 3.17 eV respectively, which show large blue shift from bulk ZnSe. This may be due to, as neodymium dopant concentration increases in host matrices, particle size increases (mentioned in XRD analysis) resulting decrease of the band gap value and this size distribution affect the optical band gap value [22]. It is observed from the Fig. 4.b, the percentage optical reflectance in the NIR region decreases with an increasing dopant concentration [23].

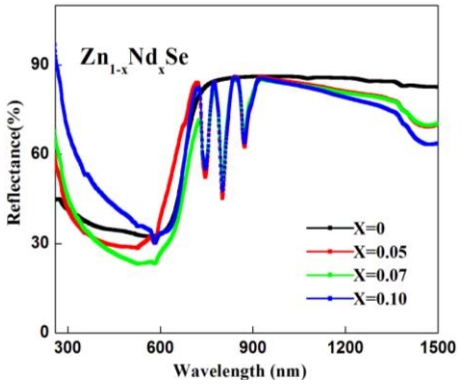

Fig. 4.b Reflectance spectra of $Zn_{1-x}Nd_xSe$ Nanoparticles

3.4 VSM analysis

Dilute magnetic semiconductor (DMS) is one of the parameters that determine ferromagnetic ordering in the materials. The VSM curve for all samples is shown in Fig. 5. The hysteresis loop of the sample has extremely small area and the very low coercivity value indicates a less hysteresis loss. The above feature confirms the soft magnetic behavior of the material and it`s exhibiting the superparamagnetic or weak ferromagnetic ordering. The addition of dopant ion in the host matrices introduces a local magnetic moment due to the localized 'd' electron [24].With doping of Neodymium, magnetic saturation M_s value is gradually increased and this depends on the cation distribution in lattice site as shown in Fig. 5 (inset). The decrease in coercivity value with the increase of particle size can be explained on the basis of domain structure and anisotropy of the crystal.

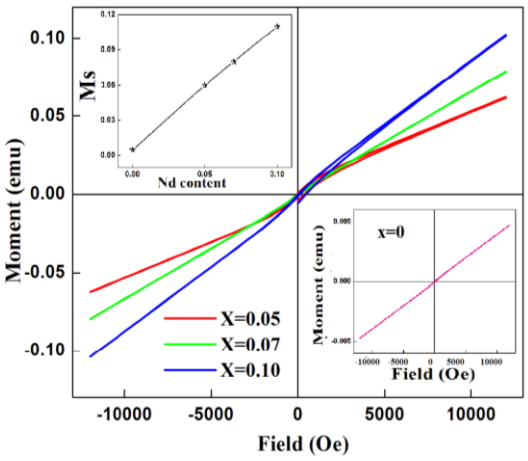

Fig. 5 VSM hysteresis curve for $Zn_{1-x}Nd_xSe$ (x= 0, 0.05, 0.07 and 0.10)

According to the exchange interaction model, the coercivity of DMS material affects the grain size [25]. As the amount of doping concentration is increased, the grain size is increased and coercivity valve decreased and it is in good agreement with XRD analysis. And it also due to the Nd^{3+} ion is situated on the octahedral B site in 4f electrons and its magnetic dipole orientation exhibits a disorder. Due to this, the exchange interaction between the sites is reduced and leads to decrease of coercive field [26].

3.5 Antibacterial activity

The antibacterial activities of undoped ZnSe and $Zn_{1-x}Nd_xSe$ (x= 0.05, 0.07 and 0.1) nanoparticle at pH 5 is shown in Fig. 6. The average value of zone of inhibition diameter against

gram positive and gram negative bacteria is presented in table. 1. It is reported that, strong activity is exhibited when the zone of inhibition is greater than 16 mm, for moderate activity zone of inhibition is lie in the range of 10-15 mm and for weak activity zone of inhibition less than 10 mm [27]. Compared to all, $Zn_{0.90}Nd_{0.10}Se$ nanoparticle is having good antibacterial activity and rest synthesis materials have moderate activity. The synthesized material has greater sensitivity of gram positive organism than gram negative organism.

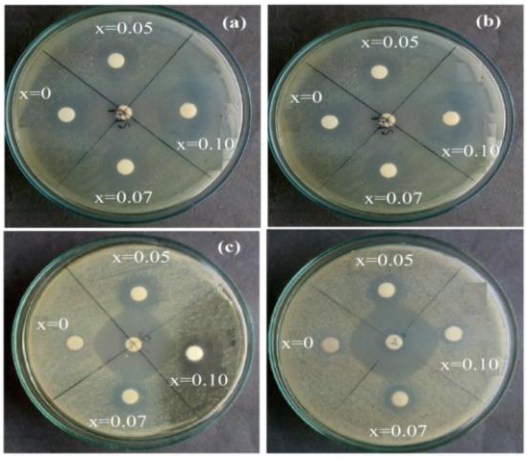

Fig. 6 Zone of inhibition on petri plates a) Staphylococcus aureus b) Bacillus substilis c) Escherichia coli d) Pseudomonas auroginosa

Table. 1 Antibacterial activity of $Zn_{1-x}Nd_xSe$ (x= 0, 0.05, 0.07 and 0.10) nanoparticles

S.no	Organisms	Zone of Inhibition (mm)				
		Std. Ciprofloxacin (10µg/disc)	Sample ($Zn_{1-x}Nd_xSe$) (100µg/disc)			
			X=0	X=0.05	X=0.07	X=0.10
1	Staphylococcus aureus	30	9	10	8	11
2	Bacillus substilis	30	10	13	8	15
3	Escherichia coli	32	7	10	7	11
4	Pseudomonas auroginosa	34	10	10	8	10

4. Conclusion

A simple and general wet chemical route was developed to synthesize cubic zinc blende ZnSe and Nd:ZnSe nanoparticles in the presence of hydrazine hydrate at pH5. Powder XRD pattern confirms the precipitated particle in nanosize and particle size increases with dopant concentration in the range of 5-25 nm. The morphology is changed from agglomerate fine powder to porous, spongy shaped with dopant concentration and this interconnects the growth kinetics of the end product. Optical absorption spectrum reveals the direct transition and energy gap decrease with dopant concentration, which may be due to the increase in crystallite size. The VSM analysis exhibits the superparamagnetic and weak ferromagnetic nature. As neodymium concentration increases, the magnetic saturation increases and coercivity value decreased. The antibacterial studies against two gram positive and gram negative bacterial strains indicate moderate activity. The outcome of these studies reveals that the above material is suitable for fabrication of nanoelectronics devices, optoelectronics and bio imaging.

Reference

[1] Z. Tang,N.A. Kotov, M. Giersig, Science **297**, 237 (2002).
[2] S. M. Lee, S. N. Cho, J. Cheon, Adv. Mater. **15**, 441 (2003).
[3] X. Peng, L. Manna, W. Yang, J. Wickham, E. Scher, A Kadavanich, A. Alivisatos, Nature . **404**, 59 (2000).
[4] J. Kimpton, T. H. RandleJ. Drennan, Solid State Ionics **149**, 89 (2002).
[5] L. A. Xue, Y. Chen, and R. J. Brook, Mater. Sci. Eng. B, **1**, 193 (1988).
[6] J. Wang, M.S. Gudiksen, X. Duan, Y. Cui, C.M. Lieber, Science **293**, 145 (2001)
[7] J. Hu, L. Li, W. Yang, L. Manna, L.-W. Wang, A. P. Alivisatos, Science **292**, 2060 (2001)
[8] R. S. Friedman, M. C. McAlpine, D. S. Ricketts, D. Ham, C. M. Lieber, Nature **434**, 1085 (2005)
[9] X. Ren, Q. Li, Y. Xue, X. Zhai, M. Yu, J. Colloid Interface Sci. **389**, 53 (2013)
[10] I. Nasieka, M. Boyko, V. Strelchuk, N. Kovalenko, A. Gerasimenko, N. Starzhinskiy, A. Zhukov, I. Zenya, D. Sofronov, Opt. Mater. (Amst). **38**, 272 (2014)
[11] K. Saikia, P. Deb, E. Kalita, Curr. Appl. Phys, **13**, 925 (2013)
[12] H. Gong, H. Huang, L. Ding, M. Wang, K. Liu, J. Cryst. Growth, **288**, 96 (2006)
[13] J. Yang, G. Wang, H. Liu, J. Park, X. Gou, X. Cheng, J. Cryst. Growth, **310**, 3645 (2008)
[14] S. R. D. Saravanakkumar, M. Kashif, V. Rethinasami, B. Ravikumar , S. Pandiarajan, A. Ayeshamariam, S. Sivaranjani, M. Bououdina, J. Ovonic Res. **10**, 175 (2014)
[15] R. Xie, X. Zhang, H. Liu, Mater. Sci. Eng. B,**182**, 86 (2014)
[16] L. Guo, S. Yang, C. Yang, P. Yu, J. Wang, W. Ge, G. K. L. Wong, Appl. Phys. Lett. **76**, 2901 (2000)
[17] K. Yadav, Y. Dwivedi, N. Jaggi, J. Lumin. **158**, 181 (2015)
[18] W. Feng, H. Zhou, F. Chen, Vacuum **114**, 82 (2015)
[19] P. Kumar, J. Singh, M. K. Pandey, C.E. Jeyanthi, R. Siddheswaran, M. Paulraj, K.N. Hui, K.S. Hui, Mater. Res. Bull. **49**, 144 (2014)
[20] P. Kumar, K. Singh, J. Lumin. **130**, 2026 (2010)
[21] A. Wei, X. Zhao, J. Liu, Y. Zhao, Phys. B, **410**, 120 (2013)
[22] M. Halajan, M. J. Torkamany, D. Dorranian, J. Physics and Chemistry of solids **75**, 1187 (2014)
[23] K. C. Preetha, T. L. Remadevi, Mater. Sci in Semicond. Proces. **39**, 178 (2015)
[24] J. N. Eckstein, Handbook of Magnetism and Advanced Magnetic Materials. John Wiley & Sons, Ltd. 322, (2007)
[25] G. Herzer, J. Magn. Magn. Mater. **112**, 258 (1992)
[26] C. Srinivas, B. V. Tirupanyam, A. Satish, V. Seshubai, D. L. Sastry, O. F. Caltun, J. Magn. Magn. Mater.**382**, 15 (2015)
[27] Z.H. Chohan, M.M. Naseer, Appl. Organomet. Chem. **21**, 728 (2007).